THERMAL DIFFUSION EFFECTS ON TRANSIENT FREE CONVECTIVE MAGNETI-NANO FLUID IN THE PRESENCE OF THERMAL RADIATION

[1] B.Seshaiah
Department of Mathematics,
Santhiram Engineering College, Nandyal
[2] S.Nazia
Research Scholar, Department of Mathematics,
Jawaharlal Nehru Technological University, Anantapuramu, A.P, INDIA.

ABSTRACT: The heat and mass transfer effects on MHD flow of an incompressible, electrically conducting, viscous fluid past an infinite moving vertical porous plate along with porous medium in the presence of radiation and thermal diffusion is investigated. It is considered that the influence of the uniform magnetic field acts normal to the flow. The water-based nano-fluid consisting copper is taken into consideration. The nano particles are restricted to spherical shape. The problem along with boundary conditions are solved by trail solution method. We have analyzed the non-dimensional fluid velocity at forth movement of the plate and the numerical values of the non-dimensional skin-friction are presented for stationary plate and moving plate. The present results are compared with the existing literature and found a good agreement for the reduced cases.

Keywords: Moving vertical porous plate, Soret effect, Nano-fluid and Thermal radiation.

INTRODUCTION

Nanofluids have many applications in the industries because of their unique physical and chemical properties. Magnetohydrodynamic (MHD) flow with heat and mass transfer has essential applications for real world problems in physics, chemistry and engineering. In recent years, the concept of a nanofluid has been proposed as a route for enhancing the performance of the heat transfer rates in the liquids. Materials, with sizes of nanometers possess unique physical and chemical properties. They can flow smoothly through micro channels without clogging because they are sufficiently small to behave similar to liquid molecules analyzed by khanafer et al. [11]. This fact has attracted much research into the investigation of the heat transfer characteristics in nanofluids. It has been found that the presence of nanoparticles within the fluid can appreciably increase the effective thermal conductivity of the fluid and, as a consequence, enhance the heat transfer characteristics. Makinde and Aziz [1] performed the boundary layer problems of stagnation point flow over a stretching or shrinking sheet. Sheikholeslami and Rashidi [2] employed heat transfer effects on nanofluids and in presence of magnetic field. Convective nanofluids flow of stretching sheet or shrinking sheet with thermal and solutal boundary conditions was studied by Uddin et al. [3]. Chamkha and Aly [4] utilized MHD free convection of a nanofluid flow in the presence of heat source or sink effects past a vertical plate. Uddin et al. [5] applied finite element method to simulate two dimensional steady state laminar boundary layer flow of a viscous electrically-conducting nanofluid in the vicinity of a stretching/shrinking porous flat plate located in a Darcian porous medium. The problem of magnetohydrodynamics boundary layer flow and heat transfer on a permeable stretching surface in a nanofluid under the effect of heat generation and partial slip analyzed by Bhargava et al. [6]. Zaimi et al. [7] studied heat transfer and boundary layer flow of a nanofluid over a stretching/shrinking sheet. Kakaç and Pramuanjaroenkij [9] examined review of convective heat transfer enhancement with nanofluids. Kandasamy et al. [10] analyzed the impact of thermophoresis particle deposition and Brownian diffusion motion on nanofluid in the presence of magnetic field and it is predicted that the magnetic strength plays a significant role on the nanoparticles in the presence of base fluid. Recently, many researchers Satyanarayana and Harish Babu [12]; Satyanarayana et al., [13]; Sheikholeslami et al., [14]; Xu et. al., [15]; Seth and Mishra [17] explained the flow and heat transfer characteristic of Newtonian/non-Newtonian nanofluids. Vedavathi et al., [19] discussed the radiation absorption, heat source and diffusion thermo effect on MHD nanofluid.

Keeping in view the above examinations, we endeavored to think about the qualities of magneto hydrodynamic free convective nanofluid

stream past a moving vertical plate within the sight of radiation and thermal diffusion. We have expanded crafted by Das and Jana (2015) with the curiosity of thinking about the mass diffusion and thermal diffusion. The water-based nanofluid containing nanoparticles of copper (Cu) have been considered in the flow contemplate.

FORMULATION OF THE PROBLEM

Thermal radiation and diffusion effects on unsteady MHD nano-fluid flow of a viscous incompressible fluid past along a vertical moving plate with an impulsive motion has been examined.

- The x^* – axis is taken along the plate in the vertical upward direction and the y^* – axis is taken normal to the plate.
- Initially it is assumed that the plate and fluid are at the same temperature T_∞^* in the stationary condition with concentration level C_∞^* at all the points.
- At time $t > 0$, the plate is given an oscillatory motion in its own plane with velocity λu_0.
- At the same time the plate temperature is raised linearly with time and also mass is diffused from the plate linearly with time.
- A transverse magnetic field of uniform strength B_0 is assumed to be applied normal to the plate. The induced magnetic field and viscous dissipation is assumed to be negligible as the magnetic Reynolds number of the flow is taken to be very small.
- The plate coincides with the plane y = 0 and the fluid flow being restricted to y > 0. It has assumed that a radiative heat flux (q_r) is applied in the normal direction to the plate.
- The fluid is water-based nanofluid containing spherical nanoparticles of Copper (Cu).
- Also it has assumed that the base fluid and the suspended nanoparticles are in thermal equilibrium.
- Thermo-physical properties of the cu-water nanofluid are shown in Table1.
- The fluid considered here is gray, absorbing/emitting radiation but a non-scattering medium.

The unsteady nanofluid boundary layer flow is governed by the following equations (see Chandra Reddy et al., [18]).

$$\rho_{nf}\, u^*_{t^*} = \mu_{nf}\, u^*_{y^*y^*} + g(\rho\beta)_{nf}(T^* - T_\infty^*) + g(\rho\beta^*)_{nf}(C^* - C_\infty^*) - \sigma_{nf} B_0^2 u^* \quad (1)$$

$$(\rho C_p)_{nf}\, T^*_{t^*} = k_{nf} T^*_{y^*y^*} - q^*_{ry} \quad (2)$$

$$C^*_{t^*} = D C^*_{y^*y^*} + D_1 T^*_{y^*y^*} \quad (3)$$

The initial and boundary conditions are

$$\left.\begin{aligned} &u^* = 0, T^* = T_\infty^*, C^* = C_\infty^* \quad for \quad all\ y^* \geq 0\ (t^* = 0) \\ &u^* = \lambda u_0, T^* = T_w^*, C^* = C_w^* \quad at\ y^* = 0 \\ &u^* \to \infty, T^* \to T_\infty^*, C^* \to C_\infty^* \quad as\ y^* \to \infty \end{aligned}\right\} (t^* > 0) \quad (4)$$

Where λ indicates the direction of the moving of the plate.

Table.I. Thermo physical properties of the base fluid and the nanoparticles Sheikholeslami et. al., [8] and Oztop and Abu-Nada [16].

Physical properties	Base fluid (Water)	Copper (Cu)
Cp (J/kgK)	4,179	385
ρ (Kg/m^3)	997.1	8,933
k (W/mK)	0.613	401
β × 10^5 (K^{-1})	21	1.67
σ(S/m)	5.5x10^{-6}	59.6x10^6

Nanofluid expressions are considered from (see Chandra Reddy et al., [18])

$$\mu_{nf} = \mu_f (1-\phi)^{-2.5},$$
$$\rho_{nf} = (1-\phi)\rho_f + \phi\rho_s,$$
$$(\rho C_p)_{nf} = (1-\phi)(\rho C_p)_f + \phi(\rho C_p)_s,$$
$$(\rho\beta)_{nf} = (1-\phi)(\rho\beta)_f + \phi(\rho\beta)_s,$$
$$(\rho\beta^*)_{nf} = (1-\phi)(\rho\beta^*)_f + \phi(\rho\beta^*)_s,$$
$$\frac{\sigma_{nf}}{\sigma_f} = \left[1 + \frac{3(\sigma-1)\phi}{(\sigma+2) - (\sigma-1)\phi}\right], \quad \sigma = \frac{\sigma_s}{\sigma_f} \quad (5)$$

The nanoparticles of spherical shape and accounted for in Eq. (5). The effective thermal conductivity of the nanofluid given by Hamilton and Crosser model followed by Kakac and Pramuanjaroenkij [9] is given by

$$\frac{k_{nf}}{k_f} = \frac{k_s + 2k_f - 2\phi(k_f - k_s)}{k_s + 2k_f + \phi(k_f - k_s)} \quad (6)$$

The radiation heat flux q_r [20] is given by

$$q_r = -\frac{4\sigma^*}{3k^*} T_y^4 \quad (7)$$

Where σ* is the Stefan-Boltzmann constant and k* is the Rosseland mean absorption coefficient. Assuming small temperature difference, it is possible to approximate

$$T^4 \approx 4T_\infty^3 T - 3T_\infty^4$$

(8)

Using (7) and (8), Eq. (2) gives

$$(\rho C_p)_{nf} T^*_{t^*} = \left(k_{nf} + \frac{16\sigma^* T_\infty^3}{3k^*} \right) T^*_{y^* y^*}$$

(9)

The transformations are adopted from [18].
The dimensionless reduced equations using above all results

$$u_t = a_1 u_{yy} + a_2 Gr\theta + a_5 Gc\, C - a_3 M^2 u$$

(10)

$$\theta_t = a_4 \theta_{yy}$$

(11)

$$ScC_t = C_{yy} - ScS_o\theta_{yy}$$

(12)

The corresponding initial and boundary conditions are

$$\left.\begin{array}{ll} u = 0, C = 0, \theta = 0 & for\ all\ y \geq 0 (t = 0) \\ u = \lambda, C = 1, \theta = 1 & at \quad y = 0, \\ u \to 0, C \to 0, \theta \to 0 & as \quad y \to \infty \end{array}\right\} (t > 0)$$

(13)

NANOFLUID EXACT SOLUTIONS

In order to reduce the above system of partial differential equations to a system of ordinary differential equations in dimensionless form, we assume the trial solution for the velocity, temperature and concentration as:

$$u(y,t) = F_0(y)e^{nt}$$

(14)

$$\theta(y,t) = G_0(y)e^{nt}$$

(15)

$$C(y,t) = H_0(y)e^{nt}$$

(16)

Substituting (14)-(16) in (10)-(12), we get

$$F_0'' - \xi_3^2 F_0 = -L_3 G_0 - L_4 H_0$$

(17)

$$G_0'' - \xi_1^2 G_0 = 0$$

(18)

$$H_0'' - \xi_2^2 H_0 = -ScS_0 G_0''$$

(19)

Here the primes denote the differentiation with respect y.
The corresponding boundary conditions are

$$\begin{array}{ll} F_0 = \lambda e^{-nt}, G_0 = e^{-nt}, H_0 = e^{-nt} & at\ y = 0 \\ F_0 \to 0, G_0 \to 0, H_0 \to 0 & as \quad y \to \infty \end{array}$$

(20)

The analytical solutions of equations (17)-(19) satisfying with the boundary conditions (20) are given by

$$F_0(y) = [L_7 e^{-\xi_3 y} + L_5 e^{-\xi_1 y} - L_6 e^{-\xi_2 y}]e^{-nt}$$

(21)

$$G_0(y) = e^{-\xi_1 y} e^{-nt}$$

(22)

$$H_0(y) = [L_2 e^{-\xi_2 y} - L_1 e^{-\xi_1 y}]e^{-nt}$$

(23)

In view of the above solutions, the velocity, temperature and concentration distributions in the boundary layer becomes

$$u(y,t) = F_0(y)e^{nt}$$

(24)

$$\theta(y,t) = G_0(y)e^{nt}$$

(25)

$$C(y,t) = H_0(y)e^{nt}$$

(26)

The local wall shear stress, the local surface heat flux and the local surface mass flux are given by

$$C_f = -(u_y)_{y=0} = \xi_3 L_7 + \xi_1 L_5 - \xi_2 L_6$$

(27)

$$Nu = -(\theta_y)_{y=0} = \xi_1$$

(28)

$$Sh = -(C_y)_{y=0} = \xi_2 L_2 - \xi_1 L_1$$

(29)

RESULTS AND DISCUSSIONS

In order to obtain the physical significance of the problem, we have plotted velocity, temperature and concentration as well as tabulated for skin-friction, the rate of heat and mass transfer for different values of physical parameters such as Grashof number(Gr), modified Groashof number(Gc), Radiation parameter(Nr), Prandtl number(Pr), Magnetic parameter(M), volume fraction parameter (ϕ), Schmidt number(Sc) and Soret number(S_0). In the present study the following default parameter values are adopted: Pr = 0.71, Nr = 0.1, ϕ = 0.05, n = 1, Sc = 0.78, S_0 = 1, λ = 1, Gr = 5, Gc = 5, M = 5 and t = 1. Therefore all graphs correspond to these values unless specifically indicated on the appropriate graph. Fig. 1 displays the effect of Schmidt number on fluid velocity. As Schmidt number increases, fluid velocity decreases. The influence of Soret number on velocity field has demonstrated in Fig. 2. It is clear that the velocity enhances with the rising values of Soret number. It is observed from Fig. 3 that the velocity decreases with increasing values of Prandtl number. This is because the fluid of low Prandtl number has high thermal diffusivity and hence attains higher temperature in steady state, which in

turn means more buoyancy force. From figure.4, we can observe that the effect of volume fraction of the nanoparticles on the nanofluid velocity profile. It is noticed that the velocity decreases with increasing of ϕ. The effect of radiation parameter Nr on the velocity has demonstrated in Fig. 5. The velocity of the fluid enhances as the value of Nr increases. The velocity distribution increase sharply near the surface of the plate. Therefore, Nr behaves like a supporting force that accelerates the fluid particles near the vicinity of the plate. Fig. 6 reveals that the fluid velocity accelerates for increasing values of magnetic parameter. The momentum boundary layer thickness decreases for increasing values of M. This trend is due to fact that the transverse magnetic field sets in Lorentz force, which The Schmidt number embodies the ratio of the momentum diffusivity to the species (mass) diffusivity. It physically relates to the comparative thickness of the hydrodynamic boundary layer and mass-transfer boundary layer. It is observed that the velocity field decreases when retards the fluid velocity. Figure 7 presents the effect of Grashof number on velocity distribution. It is noticed that the velocity u increases with increasing values of Grashof number Gr. This behavior is because the positive Grashof number Gr acts like a favorable pressure gradient that accelerates the fluid in the boundary layer. Fig. 8 displays the effect of Grashof number of mass transfer on velocity. It is observed that the velocity increases for increasing values of Gc. This occurs because of the presence of thermal and solutal buoyancy, which has the tendency of increase in velocity. The effect of Prandtl number on the variation of fluid temperature has exhibited in Fig. 9. It has noticed that the fluid temperature falls down as the Prandtl number enlarges. It is obvious that a higher Prandtl number fluid has relatively low thermal conductivity, which causes a reduction in the conduction and there by the thermal boundary layer thickness. As a result, the fluid temperature decreases. Fig. 10 represents the influence of solid volume fraction on temperature variations. It is clear that the fluid temperature rises with enlarging values of volume fraction parameter. The thermal boundary layer for Cu–water nanofluid is higher than for pure water ($\phi = 0$) since copper has more thermal conductivity and its addition to the water based fluid increases the thermal conductivity for the fluid. Hence, the thickness of the thermal boundary layer enhances. This trend coincides with the physical nature of nanoparticles. Figure 11 illustrates the effect of radiation parameter Nr on the temperature distribution. The fluid temperature increases as the value of Nr enlarges. The increase in radiation parameter corresponds to the release of heat energy from the flow region. A decrease in the values of Nr for given k_{nf} and T_∞ means a decrease in the Rosseland radiation absorptive k*. Since divergence of the radiative heat flux increases, k* decreases which in turn causes to increase the rate of radiative heat transfer of the fluid and so the fluid temperature increases. Figures 12 and 13 represent the influence of Schmidt number and Soret number on the species concentration. It is seen that the concentration field become thinner under the effect of Schmidt number, but a reverse trend has noticed in the case of Soret effect. Figure 14 shows the effect of Prandtl number on concentration profile. As the parameter increases near the boundary layer, the concentration is also increases. Fig. 15 reveals the variation of the concentration distribution under the influence of volume fraction parameter. It has observed that the fluid concentration decreases as the solid volume fraction increases. The fluid concentration becomes thinner with increasing values of radiation parameter. It is clearly shown in Fig. 16.

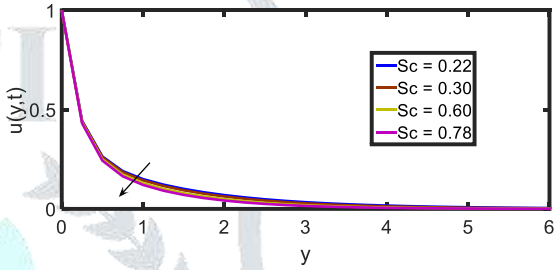

Fig. 1. Velocity profiles for various values of Schmidt number(Sc)

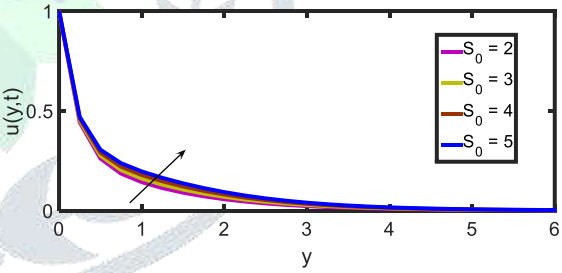

Fig. 2. Velocity profiles for various values of Soret number(S_0)

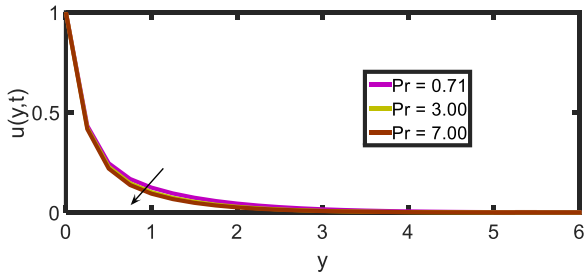

Fig. 3. Velocity profiles for various values of Prandtl parameter(Pr)

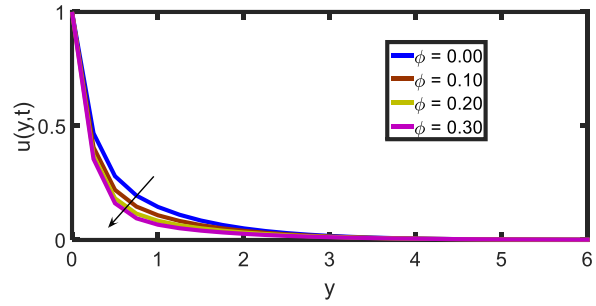

Fig. 4. Velocity profiles for various values of Solid volume fraction (ϕ)

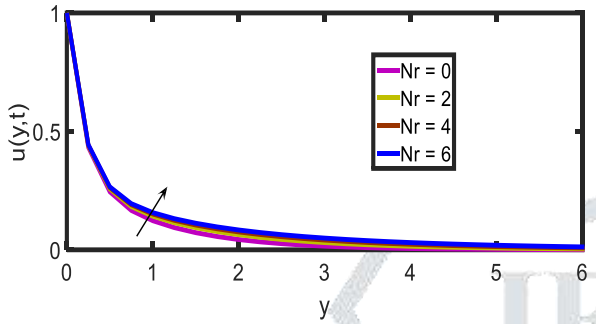

Fig. 5. Velocity profiles for various values of radiation parameter (Nr)

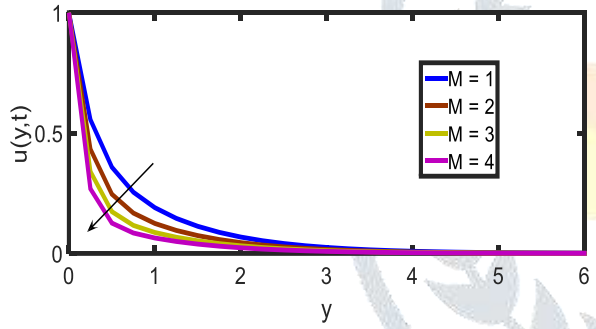

Fig. 6. Velocity profiles for various values of Magnetic parameter(M)

Numerical results of the non-dimensional skin friction are presented in Table. 2-9 under the effects of Grashof number(Gr), modified Groashof number(Gc), Radiation parameter(Nr), Prandtl number(Pr), Magnetic parameter(M), volume fraction parameter (ϕ) Schmidt number(Sc) and Soret number(S_0).

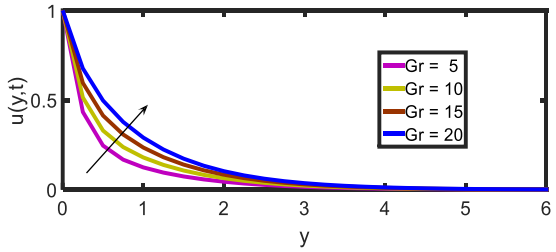

Fig. 7. Velocity profiles for various values of Grashof Number(Gr)

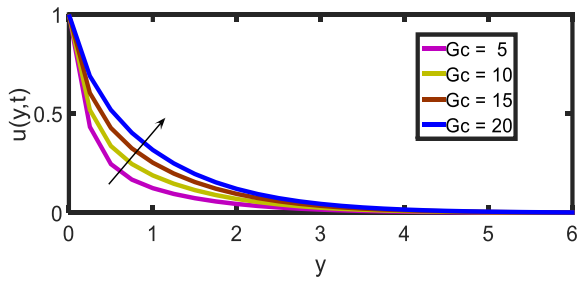

Fig. 8. Velocity profiles for various values of modified Grashof Number(Gc)

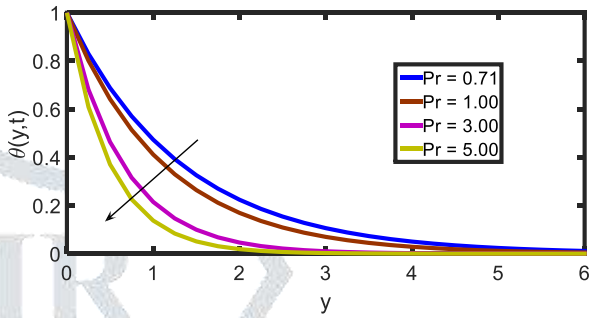

Fig. 9. Temperature profiles for various values of Prandtl parameter(Pr)

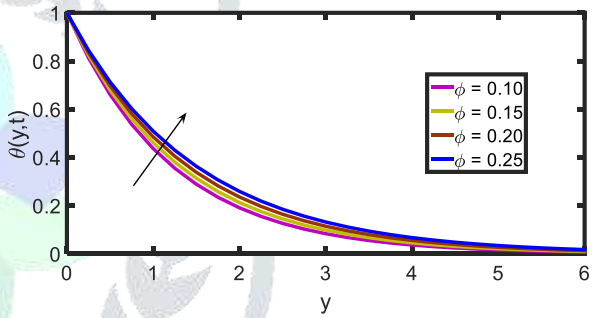

Fig. 10. Temperature profiles for various values of Solid volume fraction (ϕ)

The effects of the Radiation parameter(Nr), Soret number(S_0), Grashof number(Gr) and modified Groashof number(Gc) reduces for increasing values of both the numbers for the tationary plate (λ = 0) and also moving plate (λ = ±1). Also The effects of the prandtl number(Pr), Magnetic parameter(M), Schmidt number(Sc) and volume fraction parameter (ϕ) enhances for increasing values of both the numbers for the stationary plate (λ = 0) and also moving plate (λ = ±1).

Numerical results of the non-dimensional Nusselt number are presented in Table.10. From Table 10 it is evident that the rate of heat transfer reduced with the increasing values of radiation parameter. This happens because as thermal radiation increases, the dominance effect of temperature gradient decreases. As the Prandtl number increases the rate of heat transfer enhances. It is evident from Table 10 illustrates that the rate of heat transfer increases as volume fraction parameter decreases. This has been

realized with the decrease in thermal conductivity under the effect of solid volume fraction of nano particles.

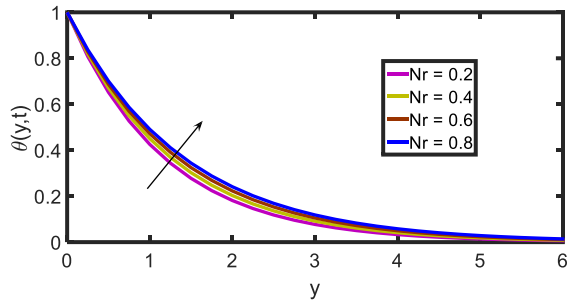

Fig. 11. Temperature profiles for various values of radiation parameter (Nr)

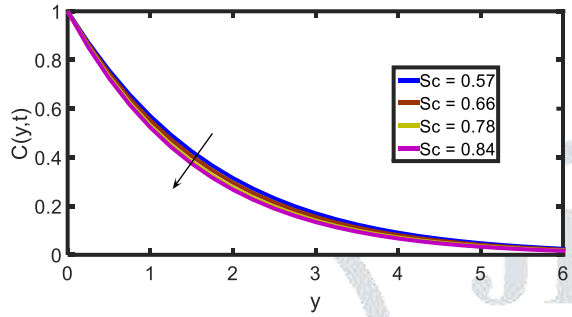

Fig. 12. Concentration profiles for various values of Schmidt number(Sc)

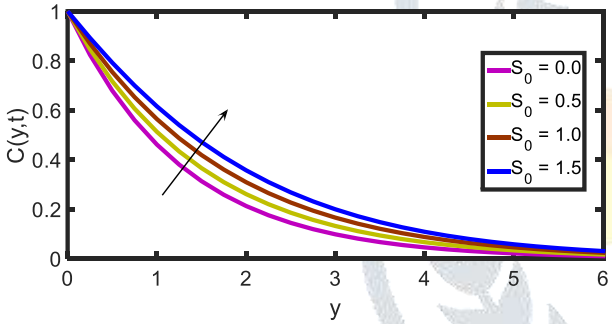

Fig. 13. Concentration profiles for various values of Soret number(S_0)

Numerical results of the non-dimensional Sherwood number are presented in Table. 11. The effects on the non-dimensional rate of mass transfer at the plate y = 0 are shown in Table 11 for several values of Soret number So, Schmidt number Sc, radiation parameter Nr, Prandtl number(Pr) and volume fraction parameter ϕ. The effects of the Radiation parameter (Nr), Schmidt number(Sc) and volume fraction parameter (ϕ) enhances for increasing values of both the numbers. The effects of the Soret number (S_0) and Prandtl number (Pr) reduces for increasing values of both the numbers.

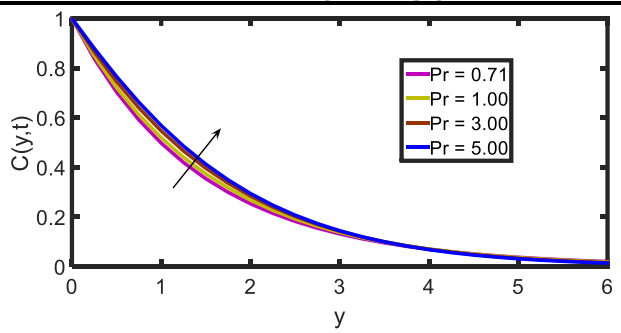

Fig. 14. Concentration profiles for various values of Prandtl parameter(Pr)

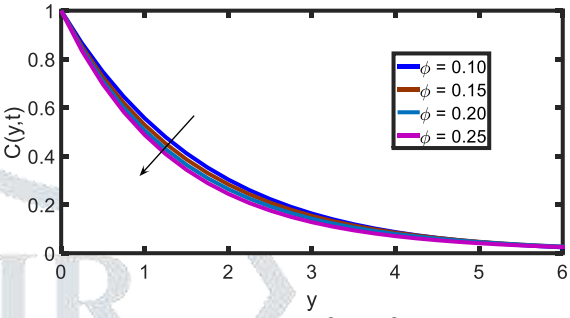

Fig. 15. Concentration profiles for various values of Solid volume fraction (ϕ)

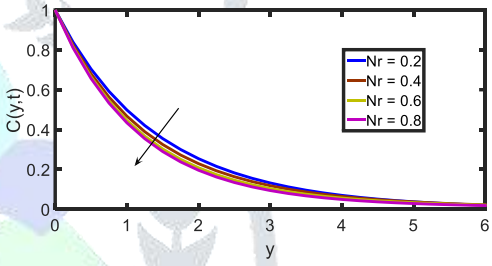

Fig. 16. Concentration profiles for various values of radiation parameter (Nr)

Table.II. Skin-friction values for various values of radiation parameter (Nr)

Nr	**λ = 1(back movement of the plate)**	**λ = 0 (stationary plate)**	**λ = 1(forth movement of the plate)**
0.2	- 6.6584	- 1.4919	3.6747
0.3	- 6.6603	- 1.4938	3.6728
0.4	- 6.6621	- 1.4955	3.6710
0.5	- 6.6637	- 1.4971	3.6694

Table.III. Skin-friction values for various values of Soret number(S_0)

S_0	λ = -1(back movement of the plate)	λ = 0(stationary plate)	λ = 1(forth movement of the plate)
2	-6.6835	-1.5170	3.6496
3	-6.7108	-1.5442	3.6223
4	-6.7380	-1.5714	3.5951
5	-6.7652	-1.5986	3.5679

Table.IV. Skin-friction values for various values of Solid volume fraction (ϕ)

ϕ	λ = -1(back movement of the plate)	λ = 0(stationary plate)	λ = 1(forth movement of the plate)
0.10	-6.4749	-1.2793	3.9163
0.15	-6.2857	-1.0963	4.0932
0.20	-6.0868	-0.9363	4.2141
0.25	-5.8768	-0.7961	4.2846

Table.V. Skin-friction values for various values of Magnetic parameter (M)

M	λ = -1(back movement of the plate)	λ = 0(stationary plate)	λ = 1(forth movement of the plate)
1	-2.3038	-0.8044	0.6950
2	-2.8892	-0.5862	1.7168
3	-3.6715	-0.4471	2.7773
4	-4.5447	-0.3583	3.8282

Table.VI. Skin-friction values for various values of Grashof numner(Gr)

Gr	λ = -1(back movement of the plate)	λ = 0(stationary plate)	λ = 1(forth movement of the plate)
1	-6.0700	-0.9035	4.2631
2	-6.2166	-1.0500	4.1165
3	-6.3632	-1.1966	3.9699
4	-6.5097	-1.3432	3.8233

Table.VII. Skin-friction values for various values of modified
Grashof numner(Gc)

Gc	λ = -1(back movement of the plate)	λ = 0 (stationary plate)	λ = 1(forth movement of the plate)
1	- 6.0508	- 0.8843	4.2823
2	- 6.2022	-1.0357	4.1309
3	- 6.3536	-1.1870	3.9795
4	- 6.5050	-1.3384	3.8281

Table.VIII. Skin-friction values for various values of
Prandtl number (Pr)

Pr	λ = -1(back movement of the plate)	λ = 0(stationary plate)	λ = 1(forth movement of the plate)
1	-6.6465	-1.4799	3.6866
2	-6.6241	-1.4576	3.7090
3	-6.6096	-1.4430	3.7235
4	-6.5986	-1.4321	3.7345

Table.IX. Skin-friction values for various values of Schmidt number (Sc)

Sc	λ = -1(back movement of the plate)	λ = 0(stationary plate)	λ = 1(forth movement of the plate)
0.22	-6.0152	-1.8287	2.3577
0.30	-6.0047	-1.8182	2.3682
0.60	-5.9778	-1.7913	2.3951
0.78	-5.9664	-1.7800	2.4065

CONCLUSIONS

The problem of thermal diffusion effects on transient free convective magneto-nanofluid flow in the presence of thermal radiation effects has been analyzed. In this paper we considered Cu-water nanofluid and the nanoparticles are in spherical shape.

- The fluid velocity increases with increasing radiation parameter and Soret number whereas opposite trend is shown in the case of Prandtl number and Schmidt number.
- An increase in radiation parameter and solid volume fraction leads to enhance the fluid temperature.

- Rising values of Soret number serves to improve the species concentration.
- Increasing values of Schmidt number enhanced the shear stress at the plate but a reverse trend is noticed in the case of Soret number.

Table.X. Nusselt number for various parameters

Nr	Pr	ϕ	Nu
0.2			0.7201
0.3			0.6950
0.4			0.6723
0.5			0.6517
	1		0.8880
	3		1.5380
	5		1.9856
	7		2.3494
		0.10	0.9680
		0.15	0.6520
		0.20	0.6093
		0.25	0.5695

Table.XI. Sherwood number for various parameters

S_0	Sc	Nr	Pr	ϕ	Sh
0.1					0.7525
0.2					0.7305
0.3					0.7084
0.4					0.6864
	0.22				0.3679
	0.30				0.4181
	0.60				0.5540
	0.78				0.6155
		0.2			0.5664
		0.3			0.5774
		0.4			0.5872
		0.5			0.5959
			1		0.4900
			2		0.3806
			3		0.1609
			4		0.0326
				0.10	0.5761
				0.15	0.5958
				0.20	0.6136
				0.25	0.6298

NOMENCLATURE

B_0 magnetic field (Am^{-1});
u* velocity component along the x-direction(ms^{-1});
C_f skin friction coefficient;
C* concentration (g/ml);
Cp specific heat at constant pressure ($jkg^{-1}K^{-1}$);
μ_{nf} dynamic viscosity of the nano fluid (Pas);
g gravitational acceleration (ms^{-2});
ρ_{nf} density of the nanofluid (kgm^{-3});
k thermal conductivity ($Wm^{-1}K^{-1}$);
σ_{nf} electrical conductivity of the nanofluid($ohm^{-1}s^{-1}$);
M magnetic strength parameter;
k_{nf} thermal conductivity of the nanofluid ($Wm^{-1}K^{-1}$);
Nu Nusselt number;
$(\rho Cp)_{nf}$ heat capacitance of the nano fluid;
Nr radiation parameter;
β_{nf} thermal expansion coefficient(K^{-1});
Pr Prandtl number;
β^*_{nf} mass transfer coefficient (m/s);
q_r heat flux by radiation(Wm^{-2});
ϕ solid volume fraction of the nano particle (mg);
q_w heat flux(Wm^{-2});
ρ_f density of the base fluid(kgm^{-3});
T* temperature of the fluid (K);
ρ_s density of the nanoparticles;
t dimensional time (sec);
β thermal expansion coefficient (K^{-1});
μ dynamic viscosity ($kgm^{-1}s^{-1}$);
ν kinematic viscosity (m^2s^{-1});
ρ density (kgm^{-3});
σ electrical conductivity(Sm^{-1});
σ* Stefan-Boltzmann constant($Wm^{-2}K^{-4}$);
σ_f electrical conductivity of the base fluid ($ohm^{-1}s^{-1}$);
σ_s electrical conductivity of the nanoparticles;
μ_f viscosity of the base fluid (pas);
$(\rho Cp)_f$ heat capacitance of the base fluid;
$(\rho Cp)_s$ heat capacitance of the nano particles;
D mass diffusion coefficient;
D_1 thermal diffusion coefficient;
k_f thermal conductivity of the base fluid ($Wm^{-1}K^{-1}$);
k_s thermal conductivity of the nano particles;

Subscripts:

f fluid property;
nf nanofluid;
s nanoparticle property;
w wall value;
∞ ambient value;

Superscripts:

* dimensional;

REFERENCES

[1] Makinde O. D., Aziz A., (2011). "Boundary layer flow of a nanofluid past a stretching sheet with a convective boundary condition", Int. J. Thermal Sci., 50: 1326-1332.
[2] Sheikholeslami M., Rashidi M. M., (2015). "Effect of space dependent magnetic field on free convection of Fe3O4-water nanofluid", J. Taiwan Inst. Chemical Eng., 56: 6-15
[3] Uddin Md. J., Bég O. A., Ismail A. I., (2015). "Radiative convective nanofluid flow past a stretching/shrinking sheet with slip effects", J. Thermodynamics and Heat Transf., 29: 513-523
[4] Chamkha A. J., Aly A. M., (2010). "MHD free convection flow of a Nanofluid past a vertical plate in the presence of heat generation or absorption effects", Chemical Eng. Commun., 198: 425-441.

[5] Uddin M. J., Rana P., Anwar Bég O., Ismail A. I. M., (2016). "Finite element simulation of magneto hydrodynamic convective nanofluid slip flow in porous media with nonlinear radiation", Alexandria Eng. J., 55: 1305-1319.

[6] Bhargava R., Goyal M., Pratibha, (2015). "An efficient hybrid approach for simulating MHD nanofluid flow over a permeable stretching sheet", Springer Proc. Math. Stat., 143: 701-714.

[7] Zaimi K, Ishak A, Pop I (2014) Boundary layer flow and heat transfer over a non linearly permeable stretching/shrinking sheet in a nanofluid. Appl Math Comput Biol Bioinform 4:4404.

[8] Sheikholeslami, M, Bandpy, MG, Ganji, DD, Soleimani, S, Seyyedi, SM: Natural convection of nanofluids in an enclosure between a circular and a sinusoidal cylinder in the presence of magnetic field. Int. Commun. Heat Mass Transf. 39, 1435-1443 (2012)

[9] Kakaç, S., and Pramuanjaroenkij, A., 2009, "Review of Convective Heat Transfer Enhancement with Nanofluids," International Journal of Heat and Mass Transfer, 52, 3187–3196.

[10] Kandasamy, K., Loganathan, P., and Puvi Arasu, P., 2011, "Scaling Group Transformation for MHD Boundary-Layer Flow of a Nanofluid Past a Vertical Stretching Surface in the Presence of Suction/Injection," Nuclear Engineering and Design, 241, 2053–2059.

[11] Khanafer, K., Vafai, K., and Lightstone, M., 2003, "Buoyancy-Driven Heat Transfer Enhancement in a Two-Dimensional Enclosure Utilizing Nanofluids," International Journal of Heat and Mass Transfer. 46, 3639–3653.

[12] Satya Narayana, P.V., and Harish Babu, D., 2016, "Numerical MHD Heat and Mass Transfer Jeffrey Fluid over a Stretching Sheet with Chemical Reaction and Radiation Parameter," Journal of the Taiwan Institute of Chemical Engineers, 59, 18–25.

[13] Satya Narayana, P.V., Venkateswarlu, B., and Venkataramana, S., 2015, "Thermal Radiation and Heat Source Effects on MHD Nanofluid Past a Vertical Plate in a Rotating System with Porous Medium. Heat Transfer-Asian Research, 44 (1), 1-19

[14] Sheikholeslami, M., Bandpy, M.G., Ellahi, R., and Zeeshan, A., 2014, "Simulation of MHD CuO–Water Nanofluid Flow and Convective Heat Transfer Considering Lorentz Forces," Journal of Magnetism and Magnetic Materials, 369, 69–80.

[15] Xu, H., Fan, T., and Pop, I., 2013, "Analysis of Mixed Convection Flow of a Nanofluid in a Vertical Channel with the Buongiorno Mathematical Model," International Communication in Heat and Mass Transfer, 44, 15–22.

[16] Oztop HF, Abu-Nada E. Numerical study of natural convection in partially heated rectangular enclosures filled with nanofluids. Int J Heat and Fluid Flow. 2008; 29(5):1326–36.

[17] GS Seth, MK Mishra, "Analysis of transient flow of MHD nanofluid past a non-linear stretching sheet considering Navier's slip boundary condition", Advanced Powder Technology 28 (2), 375-384, 2017.[18] P. Chandra Reddy , M.C. Raju, G.S.S. Raju , S.V.K. Varma, "Free Convective Magneto-Nanofluid Flow Past A Moving Vertical Plate In The Presence Of Radiation And Thermal Diffusion", Frontiers in Heat and Mass Transfer (FHMT), 7, 28 (2016), 1-11.[19] N. Vedavathi, G. Dharmaiah**,** K.S. Balamurugan and J. Prakash, "Heat Transfer On Mhd Nanofluid Flow Over A Semi Infinite Flat Plate Embedded In A Porous Medium With Radiation Absorption, Heat Source And Diffusion Thermo Effect", Frontiers in Heat and Mass Transfer (FHMT), 9, 38 (2017),p.p.1-8.

[20] Magyari, E., Pantokratoras, A., "Note on the effect of thermal radiation in the linearized Rosseland approximation on the heat transfer characteristics of various boundary layer flows", Int. Commun, Heat Mass Transfer, 38(5), (2011), p.p.-554-556.